

Precise dipole moments and quadrupole coupling constants of the *cis* and *trans* conformers of 3-aminophenol: Determination of the absolute conformation

Frank Filsinger,¹ Kirstin Wohlfart,¹ Melanie Schnell,¹ Jens-Uwe Grabow,² and Jochen Küpper^{1,*}

¹Fritz-Haber-Institut der Max-Planck-Gesellschaft, Faradayweg 4-6, 14195 Berlin, Germany

²Gottfried-Wilhelm-Leibniz-Universität, Institut für Physikalische Chemie und Elektrochemie, Callinstr. 3a, 30167 Hannover, Germany

(Dated: November 2, 2020)

The rotational constants and the nitrogen nuclear quadrupole coupling constants of *cis*-3-aminophenol and *trans*-3-aminophenol are determined using Fourier-transform microwave spectroscopy. We examine several $J = 2 \leftarrow 1$ and $1 \leftarrow 0$ hyperfine-resolved rotational transitions for both conformers. The transitions are fit to a rigid rotor Hamiltonian including nuclear quadrupole coupling to account for the ^{14}N nuclear spin. For *cis*-3-aminophenol we obtain rotational constants of $A = 3734.930$ MHz, $B = 1823.2095$ MHz, and $C = 1226.493$ MHz, for *trans*-3-aminophenol of $A = 3730.1676$ MHz, $B = 1828.25774$ MHz, and $C = 1228.1948$ MHz. The dipole moments are precisely determined using Stark effect measurements for several hyperfine transitions to $\mu_a = 1.7718$ D, $\mu_b = 1.517$ D for *cis*-3-aminophenol and $\mu_a = 0.5563$ D, $\mu_b = 0.5375$ D for *trans*-3-aminophenol. Whereas the rotational constants and quadrupole coupling constants do not allow to determine the absolute configuration of the two conformers, this assignment is straight-forward based on the dipole moments. High-level *ab initio* calculations (B3LYP/6-31G* to MP2/aug-cc-pVTZ) are performed providing error estimates of rotational constants and dipole moments obtained for large molecules by these theoretical methods.

PACS numbers: 33.20.Bx; 33.55.Be; 33.15.-e

Keywords: microwave spectroscopy; dipole moment; Stark effect; conformers; cold molecules; rotational spectroscopy; supersonic jet; molecular structure

I. INTRODUCTION

Since the observation of multiple conformers of tryptophan in a supersonic jet at low temperatures 20 years ago [1], such occurrence of multiple conformers (torsional isomers, rotamers) is quite common for the so called “building blocks of life under isolated conditions” [2, 3] and other modular molecules, even at the low temperatures in a cold supersonic jet. Vast progress was made on the electronic and vibrational spectroscopy of these species. Often the comparison of experimental and *ab initio* vibrational frequencies can be used to distinguish between the isomers [2, 3]. However, in many cases the structural differences are subtle, resulting in very similar vibrational spectra. Thus more sophisticated methods are required. Dong and Miller, for example, assigned individual isomers of cytosine exploiting the angles between vibrational transition moments and the permanent dipole moments of oriented cytosine [4].

Rotational spectroscopy provides precise moments of inertia (rotational constants), quadrupole coupling constants, and dipole moments, which allow for a detailed understanding of the structural and electronic properties of individual conformers. In principle, all of these parameters can be compared to results of *ab initio* calculations in order to assign the observed species to calculated structures. However, for structurally similar isomers

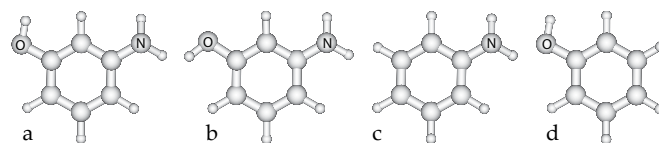


FIG. 1: Structures of (a) *cis*- and (b) *trans*-3-aminophenol, compared to (c) aniline and (d) phenol

(*vide supra*), i. e., when only the positions of some hydrogen atoms are different between the isomers, also the rotational constants cannot be used to assign the individual isomer. In such cases, the nuclear quadrupole coupling constants determined from FTMW spectroscopy have been used to discriminate between different calculated minimum structures of amino acids [5]. Similarly, the permanent dipole moments of the isomers can be used to unambiguously assign individual conformers [6]. Moreover, in principle isotopic substitution combined with a Kraitchman analysis [7] can be applied to derive conformational information. One has to carefully consider, however, that the substitution can also induce structural changes itself [8].

Here we present a detailed study of the individual conformers of 3-aminophenol (3AP) using Fourier-transform microwave spectroscopy (FTMW). 3AP exists in two distinct conformational configurations, *cis*-3-aminophenol (c3AP) and *trans*-3-aminophenol (t3AP), as shown in Figure 1. 3AP is a very interesting model system for studying primary molecular properties, because the two conformers are structurally very similar, varying only in the position of one single hydrogen

*Author to whom correspondence should be addressed. Electronic mail: jochen@fhi-berlin.mpg.de

atom, but the electronic properties are quite distinct. The two conformers have very similar rotational constants, but quite different dipole moments and, thus, Stark effects [6]. The individual conformers can also easily be selectively detected by REMPI-spectroscopy due to their different electronic properties [9, 10]. From a comparison of experimental vibrational frequencies and high-level *ab initio* calculations an assignment of the conformations was possible [9]. Moreover, 3AP is the chromophore of the essential amino acid tyrosine and closely related to dopamine, which also is a benzene derivative with a phenol group (OH) and an amino group (NH₂) substituent. From a detailed understanding of 3AP one can proceed to studies of these more complicated molecules.

The rotational spectra of the parent molecules phenol and aniline, shown in Figure 1, have been extensively studied using microwave spectroscopy, including the hyperfine structure due to the nitrogen nuclear quadrupole moment for aniline [11] and the full substitution structures [12, 13]. The dipole moments of both species were also determined using Stark effect measurements [12, 13]. For 3-aminophenol, however, to our knowledge no microwave spectroscopy investigation has been performed. The rotationally resolved electronic excitation spectrum was obtained using high-resolution laser-induced fluorescence spectroscopy and the dipole moment was determined from Stark effect measurements of these spectra [6], but this study did not provide any details on the hyperfine structure due to the nitrogen nuclear quadrupole moment.

In order to obtain the rotational constants and the dipole moment with high accuracy, we determine the rotational constants, nuclear quadrupole coupling constants, and dipole moment components of c3AP and t3AP using high-resolution FTMW spectroscopy without and with applied electric fields in the coaxially oriented beam-resonator arrangement (COBRA). We perform these measurements for the very lowest rotational states, because these states have the most sensitive Stark effect [7]. In the Stark effect measurements we give special attention to an accurate calibration of the electric field strengths, which is detailed in Appendix A.

In addition, we perform high-level *ab initio* calculations to test the quality of theoretical descriptions for these molecules. The comparisons of theoretical and experimental results will allow us to estimate the errors of theoretical rotational constants and dipole moments of similar molecules we might study in the future.

II. EXPERIMENTAL DETAILS

The experimental setup of the Hannover COBRA-FTMW-spectrometer is described in detail elsewhere [14, 15]. In brief, 3-aminophenol (purity $\geq 98\%$) was purchased from Sigma-Aldrich and used without further purification. The sample was heated to 120 °C and co-expanded in 2 bar of Ne through a pulsed nozzle (Gen-

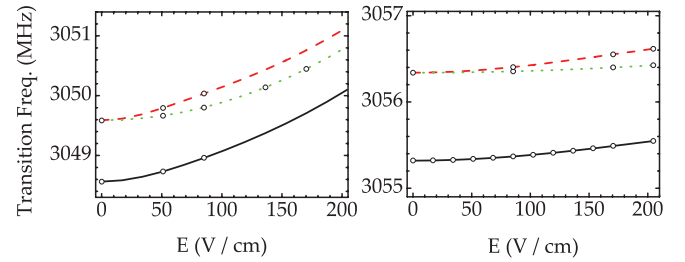


FIG. 2: (Color online:) Stark shift measurements (circles) and fitted Stark-lobes (lines) for cis-3-aminophenol (left) and trans-3-aminophenol (right). For both molecules the $J_{K_a K_c} = 1_{01} \leftarrow 0_{00}$, $F = 0 \leftarrow 1$, $m_F = 0 \leftarrow 1$ (solid black lines), $F = 2 \leftarrow 1$, $m_F = 1 \leftarrow 0$ (dashed red lines), and $F = 2 \leftarrow 1$, $m_F = 2 \leftarrow 1$ (dotted green lines) were measured.

eral Valve Series 9) with a 0.8 mm orifice. The supersonic expansion was pulsed coaxially into the microwave resonator [14], which was specially developed to provide high sensitivity and resolution at low frequencies down to 2 GHz, and the lowest rotational transitions of 3AP in the range of 3–7.5 GHz were recorded with a linewidth (FWHM) of 2.5 kHz and a frequency accuracy of 500 Hz.

Stark shift measurements were performed with the Coaxially Aligned Electrodes for Stark-effect Applied in Resonators (CAESAR) setup [15]. This setup provides a homogeneous electric field over the entire volume, from which molecules are effectively contributing to the emission signal. We calibrated the field strength using the $J = 1 \leftarrow 0$ transition of OC³⁶S (0.02% natural abundance) using a documented dipole moment of 0.71519(3) D [16], see Appendix A for details. In this way the dipole moment components were determined from several hyperfine transitions of the $J = 1 \leftarrow 0$ band measured at different electric field strengths up to 205 V/cm. The individual measurements and the respective fitted Stark lobes are shown in Figure 2.

III. COMPUTATIONAL DETAILS

We performed *ab initio* calculations of c3AP and t3AP using the Gaussian 03 program package [17]. Previously, rotational constants and dipole moments had been calculated using the B3PW91/6-31G* [6] and CASSCF and CASPT2/6-31G* [9] levels of theory. We extended these calculations to multiple methods (B3LYP, B3PW91, MP2) using the same 6-31G* and the larger aug-cc-pVTZ basis sets. We performed fully relaxed geometry optimizations of both conformers at these levels of theory and calculated the dipole moments for the obtained minimum structures on the potential energy surface. However, this procedure yielded considerable out-of-plane μ_c dipole moment components due to the non-planar structure around the nitrogen nucleus and the corresponding out-of-plane non-bonding sp^3 orbital on the nitrogen atom. These μ_c dipole moment components are, how-

$J'_{K'_a K'_c} \leftarrow J''_{K''_a K''_c}$	$F' \leftarrow F''$	comp.	obs. (MHz)	obs.-calc. (MHz)
$1_{01} \leftarrow 0_{00}$	$0 \leftarrow 1$	1	3048.5622	-0.0017
	$2 \leftarrow 1$	1	3049.5857	-0.0030
	$1 \leftarrow 1$	1	3050.2767	0.0047
$2_{02} \leftarrow 1_{01}$	$1 \leftarrow 1$	3	5978.8532	0.0009
	$3 \leftarrow 2$	1	5980.0761	-0.0005
	$2 \leftarrow 1$	1	5980.3687	0.0014
	$1 \leftarrow 0$	3	5980.5581	-0.0023
	$2 \leftarrow 2$	2	5981.0511	0.0006
$2_{12} \leftarrow 1_{01}$	$1 \leftarrow 1$	2	7412.7858	0.0020
	$3 \leftarrow 2$	3	7414.2197	-0.0024
	$2 \leftarrow 1$	2	7414.8910	0.0021
	$2 \leftarrow 2$	1	7415.5794	-0.0017

TABLE I: Measured hyperfine-split transitions for cis-3-aminophenol with fit residuals. Also the number of clearly split components is given for each transition. Note that additional splittings, which are not resolved by our spectrometer, might be present. See text for details.

ever, not experimentally observable as the zero-point vibrational level averages over all out-of-plane angles due to the inversion tunneling of the two amino hydrogen atoms. The tunneling rate is similar to the one of aniline (1 THz [11]) and much larger than the rotational frequency. To test the calculated dipole moments we also performed geometry optimizations for the planar transition states of the inversion motion for both conformers in C_s symmetry. These calculations confirmed the previous reasoning and gave in-plane dipole moment components quite similar to the specified ones. The obtained rotational constants and dipole moments are presented together with the experimental results in Section IV. For an improved theoretical description, one would need to calculate the dipole moment function along the inversion motion coordinate and derive the vibrationally averaged expectation values $\langle \mu_\alpha \rangle$, which is beyond the scope of this work.

IV. RESULTS AND DISCUSSION

The measured field-free microwave transitions of c3AP and t3AP are given in Tables I and II, respectively. For each conformer, all hyperfine transitions were fit to a rigid-rotor Hamiltonian, including nuclear quadrupole coupling for the nitrogen nucleus, using the computer program QStark [18, 19]. Several lines show additional splittings on the order of 5–10 kHz, as depicted in Figure 3 b. The number of clearly visible split components is given in Tables I and II. Many lines show additional shoulders which are not included in the Tables, as it is not possible to reliably determine them. These splittings are most likely due to magnetic spin-spin or spin-rotation coupling of the hydrogen atoms, which are not included in the used Hamiltonian. The magnetic-interaction energy of two hydrogen nuclei with parallel spins is ap-

$J'_{K'_a K'_c} \leftarrow J''_{K''_a K''_c}$	$F' \leftarrow F''$	comp.	obs. (MHz)	obs.-calc. (MHz)
$1_{01} \leftarrow 0_{00}$	$0 \leftarrow 1$	1	3055.3215	0.0021
	$2 \leftarrow 1$	1	3056.3392	-0.0001
	$1 \leftarrow 1$	2	3057.0218	0.0025
$1_{11} \leftarrow 0_{00}$	$0 \leftarrow 1$	1	4957.3704	0.0011
	$2 \leftarrow 1$	2	4958.2638	0.0006
	$1 \leftarrow 1$	1	5990.5985	0.0011
$2_{02} \leftarrow 1_{01}$	$3 \leftarrow 2$	1	5991.8183	-0.0007
	$2 \leftarrow 1$	2	5992.1126	-0.0014
	$1 \leftarrow 0$	1	5992.2975	0.0003
	$2 \leftarrow 2$	2	5992.7950	0.0010
	$3 \leftarrow 2$	1	6712.8958	-0.0016
$2_{11} \leftarrow 1_{10}$	$3 \leftarrow 2$	1	6712.8958	-0.0016
	$1 \leftarrow 1$	2	7413.1225	0.0001
	$1 \leftarrow 2$	1	7413.8012	-0.0011
$2_{12} \leftarrow 1_{01}$	$1 \leftarrow 0$	1	7414.8210	-0.0013
	$2 \leftarrow 1$	3	7415.2475	-0.0016
	$2 \leftarrow 2$	1	7415.9312	0.0022

TABLE II: Measured hyperfine-split transitions for trans-3-aminophenol with fit residuals. Also the number of clearly split components is given for each transition. Note that additional splittings, which are not resolved by our spectrometer, might be present. See text for details.

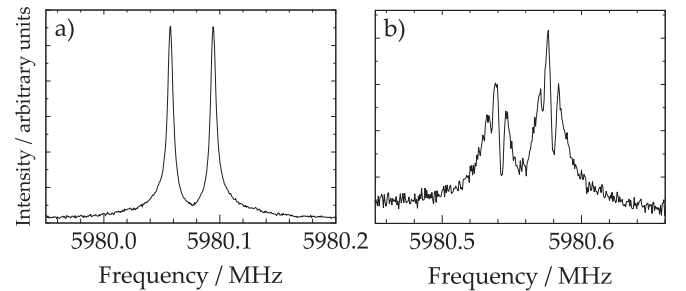


FIG. 3: Amplitude spectrum of the $J_{K_a K_c} = 2_{02}3 \leftarrow 1_{01}2$ (a) and $2_{02}1 \leftarrow 1_{01}0$ (b) hyperfine transitions for c3AP. The major doublet-splitting in both Figures is due to the Doppler-splitting in the coaxial spectrometer-arrangement. Additional splittings of the individual Doppler-components of this single quadrupole-component of the rotational transition are obvious in Figure (b). We attribute these splittings to partially resolved magnetic hyperfine structure due to the hydrogen nuclear spins; see text for details.

proximately 6 kHz for a distance of 170 pm,¹ which corresponds to the distance of the two amine hydrogen atoms. The distance between the hydroxy hydrogen to the closest hydrogen atom on the ring is 230 pm yielding a somewhat smaller interaction energy of approximately 2.5 kHz. The spin-rotation interaction of the two amine hydrogen atoms, for example, can be estimated based on the NH_3 coupling constant (18.5 kHz [20]), scaled by the relative angular velocity of ammonia ($B + C \approx 500$ GHz)

¹ The interaction energy of two magnetic dipoles is given by $W = \frac{\mu_0 \mu \mu'}{4\pi r^3}$.

and 3AP ($B + C \approx 3$ GHz). The approximately 180 times smaller angular velocity of 3AP compared to ammonia suggests couplings, which are also two orders of magnitude smaller. On the other hand, the wider charge distribution of 3AP increases the induced magnetic field and, therefore, the coupling strength. In summary, we estimate a spin-rotation coupling on the order of 1 kHz. From the number of resolved components for the different $J' \leftarrow J''$, given in Tables I and II, no systematic dependence on J can be derived. Splittings due to spin-rotation coupling are expected to increase with J , while for spin-spin coupling, one would expect a slight decrease of the splitting with increasing J [7]. Both effects are expected to result in a splitting comparable to the observed one. A detailed evaluation of these splittings would require even higher resolution measurements, the examination of higher- J transitions, or, most probably, both, in order to sufficiently resolve and analyze the underlying hyperfine structure, as has been done for ammonia [20–22]. For the purpose of this work, we determined the line-center frequencies as the intensity-weighted average of these split lines.

The fit to the experimental data is very good with remaining standard deviations of 2.93 kHz and 1.65 kHz for c3AP and t3AP, respectively. This is somewhat higher than usual, because the experimental frequencies were obtained from intensity weighting of the underlying unassigned additional hyperfine structure (*vide supra*). We want to point out that for c3AP twelve hyperfine-split lines from only three rotational transition are evaluated to yield three rotational constants and two quadrupole coupling constants. Using the QStark [18, 19] program we perform a global fit by direct diagonalization of the Hamiltonian matrix including terms for all parameters [23]. This determines well-defined values and error estimates for all five parameters simultaneously. The obtained rotational constants and quadrupole coupling constants are given in Table III. For comparison also the values determined from the high-resolution electronic excitation spectrum [6] and the *ab initio* calculated rotational constants are shown. The agreement with the previous experimental values is good. The remaining differences might be attributed to the fact that we determined the rotational constants only from transition between the very lowest rotational states, where centrifugal distortion effects are negligible. The previous electronic excitation spectroscopy experiment determined an average value over many more transitions, including transitions between much higher rotational states, where centrifugal distortion for such molecules is appreciable. Since, in that work, a rigid-rotor Hamiltonian was still used to fit the data, the thus obtained rotational constants are effective rotational constants including these centrifugal distortion effects in an averaged way.

The *ab initio* rotational constants agree reasonably well with the experimental results but show a considerable spread for the different methods and basis sets. It is obvious, that it would not be possible to determine the

absolute configuration (cis or trans) of the two conformers from comparisons of experimental and theoretical rotational constants, because the experimental constants are very similar and the potential errors of the calculated rotational constants are too large for such an assignment. The planar moments of inertia² of the vibrational ground state of $P_{cc}^0 = 0.2262 \text{ u}\text{\AA}^2$ for c3AP and $P_{cc}^0 = 0.21484 \text{ u}\text{\AA}^2$ for t3AP are comparable to the one of aniline ($P_{cc}^0 = 0.2557 \text{ u}\text{\AA}^2$ [12]). Phenol has a considerably smaller planar moment of $P_{cc}^0 = 0.01524 \text{ u}\text{\AA}^2$ [13]. These values indicate that the NH_2 configurations of c3AP and t3AP are similar to the one of aniline and no additional OH out-of-plane contributions compared to phenol are present.

The quadrupole coupling constants are also similar for the two conformers and compared to aniline [11], showing a similar chemical environment of the nitrogen nucleus in all three molecules. They would not allow to determine the absolute conformation, as was done for amino acids before [5]. We have also calculated the barriers to inversion of the amine-group at the MP2/cc-VTZ level of theory as the energy difference between the minimum energy for a planar optimized geometry (C_s -symmetry) and the absolute minimum on the PES. The barrier heights obtained in that way are 604 cm^{-1} and 567 cm^{-1} for c3AP and t3AP, respectively. For comparison we calculated the barrier for aniline at the same level of theory, which yields a value of 585 cm^{-1} in fair agreement with the experimental values of 525 cm^{-1} [24, 25] or 540 cm^{-1} [11], considering that the calculations neglect zero-point vibrational effects. Overall it is clear that the chemical environment of the amino-group is quite similar for both conformers of 3AP and for aniline.

From the Stark shift measurements we precisely determined the μ_a and μ_b dipole moment components of the two conformers by fitting the transition shifts with QStark [18, 19]. In the fitting procedure we set up and directly diagonalized the M -matrices,³ yielding an accurate description of the Stark effect for all field strengths. The experimental dipole moments are given in Table IV together with *ab initio* values. We also calculated the dipole moments of c3AP and t3AP from the dipole moments of aniline [12] and phenol [13] using simple vector addition of the individual dipole moments in the aminophenol principal axes system. These values are in excellent agreement with the experimentally observed values, confirming the dipole additivity for the ground states of 3AP [6, 26]. Using either the dipole moments predicted by the vector model or by *ab initio* calculations,

² The planar moments P_{gg} of a molecule calculate as $2 \cdot P_{gg}^v = I_{g'}^v + I_{g''}^v - I_g^v$. With $g = c, g', g'' = a, b$, and $v = 0$ we get the planar moment P_{cc} with respect to the ab -plane of the principal axes of inertia of the oblate rotors in their vibrational ground state: $2 \cdot P_{cc}^0 = I_a^0 + I_b^0 - I_c^0$

³ In all calculations the matrix dimensions in J and F exceeded their maximum values in the experimental data by 10.

method	exp. (this work)	exp. (ref. [6])	B3PW91	B3LYP	B3LYP	MP2	CASSCF(8,10) ^a
basis set			6-31G*	aug-cc-pVTZ	aug-cc-pVTZ	aug-cc-pVTZ	6-31G*
cis-3-aminophenol							
A / MHz	3734.930 (14)	3734.4 (7)	3741	3766	3728	3755	3748
B / MHz	1823.2095 (64)	1823.1 (1)	1825	1837	1817	1829	1830
C / MHz	1226.493 (11)	1226.6 (1)	1228	1236	1223	1231	1231
χ_{aa} / MHz	2.2776 (34)						
$\chi_{bb} - \chi_{cc}$ / MHz	6.179 (14)						
χ_{bb} / MHz	1.951						
χ_{cc} / MHz	-4.228						
P_{cc}^0 (uÅ ²)	0.2262 (19)	0.26(2)					
σ / MHz	0.002931	1.77					
number of lines	12	114					
trans-3-aminophenol							
A / MHz	3730.1676 (14)	3729.5 (4)	3737	3766	3723	3752	3748
B / MHz	1828.25774 (58)	1828.2 (1)	1829	1840	1821	1833	1833
C / MHz	1228.1948 (10)	1228.2 (1)	1229	1237	1224	1232	1231
χ_{aa} / MHz	2.2666 (15)						
$\chi_{bb} - \chi_{cc}$ / MHz	6.2405 (48)						
χ_{bb} / MHz	1.987						
χ_{cc} / MHz	-4.254						
P_{cc}^0 (uÅ ²)	0.21484 (18)	0.23(2)					
σ / MHz	0.001647	1.61					
number of lines	16	155					

^aPrivate communication with Markus Gerhards (2007); the values are determined from the calculations described in reference [9].

TABLE III: Rotational constant, ¹⁴N quadrupole coupling constants, planar moments of inertia P_{cc}^0 , overall standard-deviations σ of the fit, and the number of lines included in the fit for cis- and trans-3-aminophenol.

method basis set	exp. (this work)	exp. (ref. [6]) vector model	B3PW91 6-31G*	B3LYP 6-31G*	B3LYP aug-cc-pVTZ	B3LYP aug-cc-pVTZ	MP2 6-31G*	MP2 aug-cc-pVTZ	CASSCF(8,10) ^a 6-31G*	CASPT2 ^a 6-31G*
cis-3-aminophenol										
μ_a / D	1.7718 (65)	1.77 (6)	1.85	1.81	1.86	1.72	1.68	1.68	1.68	1.73
μ_b / D	1.517 (10)	1.5 (2)	1.69	1.72	1.65	1.54	1.48	1.48	1.32	1.29
$ \mu $ / D	2.333 (11)	2.3 (2)	2.51	2.50	2.49	2.31	2.14	2.14	2.14	2.16
σ / MHz	0.001294									
number of lines	10									
trans-3-aminophenol										
μ_a / D	0.5563 (17)	0.57 (1)	0.44	0.42	0.57	0.23	0.37	0.37	0.16	0.20
μ_b / D	0.5375 (32)	0.5 (1)	0.51	0.54	0.48	0.81	0.63	0.63	1.05	1.09
$ \mu $ / D	0.7735 (34)	0.7 (1)	0.67	0.68	0.75	0.84	0.73	0.73	1.06	1.11
σ / MHz	0.000890									
number of lines	19									

^aPrivate communication with Markus Gerhards (2007); the values are determined from the calculations described in reference [9]. The CASPT2 dipole moments are calculated at the CASSCF-optimized geometry.

TABLE IV: Dipole moment components μ_a and μ_b , overall dipole moments $|\mu|$ of cis- and trans-3-aminophenol, standard deviations σ of the fits, and the number of measurements at different field strengths included in the fit. See text for details.

the absolute conformation of the molecules can easily be obtained. The assignment agrees with the previous Stark effect study by Reese et al. [6]. This procedure of distinguishing conformers based on their dipole moment orientation is quite comparable to the use of vibrational transition moment angles [4]. In that work the angle between permanent dipole moment and vibrational transition dipole moments was used to distinguish different conformers. Here we use the angle between the permanent dipole moment and the principal axes for the same purpose. Overall, it is a very helpful tool to employ experimental dipole moments to determine the absolute conformational structure of modular molecules.

The quality of the *ab initio* dipole moments is quite unsatisfactory. The calculated dipole moments for the more polar conformer c3AP are typically within 10 %. For the less polar conformer t3AP the calculated values differ by considerably more than 10 % from the experimental values for all levels of theory. However, what is most discouraging for the calculation of dipole moments of large and modular molecules is the wide distribution of their calculated orientations, as can be seen from the individual components along the principal axes. Moreover, increasing the level of theory and using the larger basis set often even gives worse results. For the CASSCF calculations systematic problems in the descriptions of hydroxybenzenes due to the neglect of σ -correlation have already been described [9]. Density-functional theory (esp. the B3LYP functional) using a large basis set (aug-cc-pVTZ) gives the best overall results for the two conformers of 3AP, but it has to be more carefully examined for a wider class of molecules whether this is serendipitous or a consistent quality of this method. Overall it must be concluded, that the *ab initio* methods used here, which are applied routinely in the calculation of structures and vibrational frequencies of molecules of similar size as 3AP, perform quite poorly for the calculation of electric dipole moments of these molecules. Therefore, one has to be careful when using such *ab initio* results for the calculation of Stark shifts of large molecules, as the dipole moment components directly enter the Hamiltonian matrix calculation [7].

The dipole moments also yield important information on the intermolecular interactions of molecules. However, in a recent study of the 3AP water cluster, only a single dimer structure could be observed, an OH-OH₂ bound hydrogen structure between the t3AP conformer and water. No c3AP-water cluster was found [27]. Considering the much larger dipole moment of c3AP this indicates that the local OH-OH₂ interaction and steric effects, which are favorable for t3AP-water, are dominating over the overall electrostatic interaction. For bulk solutions, on the other hand, we would expect the more polar c3AP conformer to have a stronger interaction with the solvent than the less polar t3AP.

V. CONCLUSIONS

We measured several hyperfine-resolved rotational transitions of the conformers of 3AP for the lowest J values using FTMW spectroscopy. From a rigid rotor analysis we could precisely determine the rotational constants and ¹⁴N nuclear quadrupole coupling constants. These nuclear quadrupole coupling constants and the calculated barriers to inversion are comparable to the values of aniline, confirming a similar electronic configuration around the nitrogen nucleus. In order to assign the absolute conformation of the individual species, the rotational constants and the quadrupole coupling constants could not be used, as they are too similar for the two conformers. However, we have very precisely determined the dipole moments of both conformers using the Stark shifts of several of these lines. These dipole moments can be rationalized in terms of simple vector addition of the dipole moments of aniline and phenol, and they allow to unambiguously assign the absolute conformation, even without the need for *ab initio* calculations.

The precisely known rotational constants and dipole moment components allow us to calculate the Stark effect of the individual rotational states with good accuracy even for very high electric fields (i. e. 200 kV/cm), as applied in Alternate Gradient decelerators [28] or similar focusing devices. The Stark shifts of the two conformers are quite different, with effective dipole moments of 0.0365 cm⁻¹/(kV cm⁻¹) for c3AP and 0.0113 cm⁻¹/(kV cm⁻¹) for t3AP.⁴ Therefore one can envision to spatially separate the conformers of aminophenol or similar modular (bio-)molecules by exploiting these Stark effect differences in an m/μ -selector, similar to the m/q -selection in a mass spectrometer for charged particles.

Acknowledgments

We would like to thank Gerard Meijer for his continuous support of this work and for helpful discussions. We thank Boris Sartakov for helpful discussions on magnetic hyperfine interactions. Financial support from the Land Niedersachsen and the Deutsche Forschungsgemeinschaft, also within the priority program 1116 "Interactions in ultra-cold atomic and molecular gases", is acknowledged.

⁴ A dipole moment of 1 D corresponds to 0.0168 cm⁻¹/(kV cm⁻¹).

APPENDIX A: CALIBRATION OF THE STARK EFFECT MEASUREMENTS

The most critical factor in the determination of electric dipole moments of molecules by Stark effects measurements are accurate values of the applied electric fields. Often sufficiently homogeneous electric fields are generated by applying a voltage difference using two plane-parallel electrodes [7]. For the large volumes sampled in FTMW spectrometers this is difficult and, therefore, in the Hannover COBRA-FTMW experiment a different approach is taken: Within the CAESAR setup, the two concave mirrors of the spectrometer resonator are used as the primary capacitor electrodes and electrode rings between them are used to create a homogeneous field over a very large fraction of the resonator volume [15]. Therefore, all detected molecules experience practically the same field strength, even for the large modes at frequencies below 3 GHz.

In all such experiments the field strength must be calibrated, which is often performed in turn by Stark effect measurements for isotopologues of OCS, for which the Stark effect is known with high precision [7]. Such measurements yield an averaged effective parallel-plate separation d , which can then be used for the calculation of the electric field strength applied during other measurements performed in the same setup. In our setup, however, the cavity mirrors serve as main electrodes. For different measurement frequencies these mirrors need to be moved to fulfill the resonance conditions of the cavity. Since the effective d has a slight dependence on the mirror separation, we apply a linear correction for this

effect to all our measurements.

We first determine effective d s from Stark effect measurements on OC³⁶S, assuming a dipole moment of 0.71519 (3) D [16] and using a linear calibration curve to account for systematic errors due to a discrepancy between the displayed and the actual voltage applied to the electrodes using an FuG HCD-20000 high-voltage power supply: $U/V = 3.86(70) + 1.00203(15) \cdot U_{disp}/V$. The effective parallel-plate separation d is determined at two very different relative mirror positions, namely $z_1 = 7.12$ mm and $z_2 = 46.13$ mm. These positions are specified relative to the zero-position of the moving cavity mirror and correspond to two quite extreme translational positions of the mirror. For these z -positions we determine the effective plate separation to $d_1 = 0.58343(31)$ m and $d_2 = 0.60099(55)$ m, respectively.

For all Stark effect measurements on 3AP we then note the actual z -position and determine the effective d for that measurement by linear interpolation between the two calibration-measurements. The estimated error in the z -position of 0.01 mm for all measurements is much smaller than the error of d and has thus been neglected. In order to account for the contribution of systematic errors of the electric field strength to the total error of the dipole moments, fits were performed at the extreme values of the electric field as derived from the calibration of the voltage and of the effective plate separation (*vide supra*). These fits provide upper and lower bounds for the dipole moments of 3-aminophenol due to systematic errors, which are included in the error estimates given in Table IV.

-
- [1] T. R. Rizzo, Y. D. Park, L. Peteanu, and D. H. Levy, *J. Chem. Phys.* **83**, 4819 (1985).
- [2] R. Weinkauff, J. Schermann, M. S. de Vries, and K. Kleiner-manns, *Eur. Phys. J. D* **20**, 309 (2002).
- [3] J. P. Simons, *Phys. Chem. Chem. Phys.* **6**, E7 (2004).
- [4] F. Dong and R. E. Miller, *Science* **298**, 1227 (2002).
- [5] A. Lesarri, E. J. Cocinero, J. C. Lopez, and J. L. Alonso, *Angew. Chem. Int. Ed.* **43**, 605 (2004).
- [6] J. A. Reese, T. V. Nguyen, T. M. Korter, and D. W. Pratt, *J. Am. Chem. Soc.* **126**, 11387 (2004).
- [7] W. Gordy and R. L. Cook, *Microwave Molecular Spectra* (John Wiley & Sons, New York, NY, USA, 1984), 3rd ed.
- [8] B. M. Giuliano and W. Caminati, *Angew. Chem.* **117**, 609 (2005).
- [9] C. Unterberg, A. Gerlach, A. Jansen, and M. Gerhards, *Chem. Phys.* **304**, 237 (2004).
- [10] M. Shinozaki, M. Sakai, S. Yamaguchi, T. Fujioka, and M. Fujii, *Phys. Chem. Chem. Phys.* **5**, 5044 (2003).
- [11] B. Kleibömer and D. H. Sutter, *Z. Naturforsch. A* **43**, 561 (1988).
- [12] D. G. Lister, J. K. Tyler, J. H. Høg, and N. W. Larsen, *J. Mol. Struct.* **23**, 253 (1974).
- [13] N. W. Larsen, *J. Mol. Struct.* **51**, 175 (1979).
- [14] J.-U. Grabow, W. Stahl, and H. Dreizler, *Rev. Sci. Instrum.* **67**, 4072 (1996).
- [15] M. Schnell, D. Banser, and J.-U. Grabow, *Rev. Sci. Instrum.* **75**, 2111 (2004).
- [16] J. M. L. J. Reinartz and A. Dymanus, *Chem. Phys. Lett.* **24**, 346 (1974).
- [17] M. J. Frisch, G. W. Trucks, H. B. Schlegel, G. E. Scuse-ria, M. A. Robb, J. R. Cheeseman, J. J. A. Montgomery, T. Vreven, K. N. Kudin, J. C. Burant, et al. (2004).
- [18] Z. Kisiel, J. Kosarzewski, B. A. Pietrewicz, and L. Pszczółkowski, *Chem. Phys. Lett.* **325**, 523 (2000).
- [19] Z. Kisiel, B. A. Pietrewicz, P. W. Fowler, A. C. Legon, and E. Steiner, *J. Phys. Chem. A* **104**, 6970 (2000).
- [20] S. G. Kukolich, *Phys. Rev.* **156**, 83 (1967).
- [21] S. G. Kukolich, *Phys. Rev.* **138**, 1322 (1965).
- [22] J. van Veldhoven, J. Küpper, H. L. Bethlem, B. Sartakov, A. J. van Rooij, and G. Meijer, *Eur. Phys. J. D* **31**, 337 (2004).
- [23] D. L. Albritton, A. L. Schmeltekopf, and R. N. Zare, in *Molecular Spectroscopy: Modern Research*, edited by K. N. Rao (Academic Press, New York, NY, USA, 1976), vol. 2, chap. 1, pp. 1–67.
- [24] N. W. Larsen, E. L. Hansen, and F. M. Nicolaisen, *Chem. Phys. Lett.* **43**, 584 (1976).
- [25] R. A. Kydd and P. J. Krueger, *Chem. Phys. Lett.* **49**, 539 (1977).

- [26] D. R. Borst, T. M. Korter, and D. W. Pratt, *Chem. Phys. Lett.* **350**, 485 (2001).
- [27] M. Gerhards, A. Jansen, C. Unterberg, and A. Gerlach, *J. Chem. Phys.* **123**, 074320 (2005).
- [28] H. L. Bethlem, M. R. Tarbutt, J. Küpper, D. Carty, K. Wohlfart, E. A. Hinds, and G. Meijer, *J. Phys. B* **39**, R263 (2006).